Multiscale Science and Engineering (2020) 2:54–62
https://doi.org/10.1007/s42493-020-00035-4

ORIGINAL RESEARCH

Orientation Distribution Dependence of Piezoresistivity of Metal Nanowire-Polymer Composite

Jiyoung Jung[1] · Sangryun Lee[1] · Nicola M. Pugno[2,3,4] · Seunghwa Ryu[1]

Received: 10 December 2019 / Revised: 1 March 2020 / Accepted: 4 March 2020 / Published online: 16 March 2020

Abstract

In this study, we investigate the piezoresistivity of metal nanowire networks embedded in a polymer, which has been widely used as a highly-stretchable strain sensor, by varying the orientation distribution of nanowires. For simplicity, we assume the affine transform of the nanowire network upon stretching and compute the effective conductivity of the nanowire network by recognizing the percolation network connecting low and high voltage boundaries. Orientation-dependence is then studied firstly by varying the range of polar angle and secondly by changing the degree of alignment along loading direction. Since nanowires are embedded in thin nanowire-polymer film in most stretchable sensor applications, instead of having random orientation distribution over full solid angle, nanowires have a limited range of polar angle distribution around 90° (when the surface normal vector of a thin film is given as the zenith direction). We show that the gauge factor (relative resistance change over applied mechanical strain) decreases as the polar angle distribution gets narrower. We then study the effect of nanowire alignment on the piezoresistive response, by assuming partial alignment distribution along the tensile direction. We find that a wide range of the gauge factor, from negative to positive, appears as the initial partial alignment angle varies, and explained such response by analyzing the relative electrical path change between a pair of nanowires. Our study deepens the understanding on the percolation-network based piezoresistive sensors and provides a guideline for designing a stretchable strain sensor with the desired gauge factor.

Keywords Piezoresistivity · Percolation · Strain sensor · Nanowire · Clustering

Introduction

A strain sensor measures mechanical deformation through changes in electrical responses. With the advancement of wearable devices that are attached to various joints in a human body (such as elbows or knees), a demand on highly stretchable strain sensors rises and extensive studies have been performed to develop flexible and highly deformable sensors with high sensitivity [1–10]. One of the most promising candidates is a piezoresistive strain sensor based on metal nanowire-embedded polymer composites, which have been extensively studied experimentally and numerically [11–19]. For example, one of the most cited studies by Amjadi et al. utilized sandwiched silver nanowire-elastomer composites which shows the gauge factor of 2–14 with the maximum stretchability of 70%, with relatively small hysteresis upon loading–unloading cycle [17].

Extensive studies on the effects of volume fraction, aspect ratio, and alignment of nanowires have been performed to explore the design space (gauge factor, reproducibility, and

Electronic supplementary material The online version of this article (https://doi.org/10.1007/s42493-020-00035-4) contains supplementary material, which is available to authorized users.

✉ Seunghwa Ryu
ryush@kaist.ac.kr

1 Department of Mechanical Engineering, Korea Advanced Institute of Science and Technology (KAIST), 291 Daehak-ro, Yuseong-gu, Daejeon 34141, Republic of Korea

2 Laboratory of Bio-inspired, Bionic, Nano, Meta Materials & Mechanics, Department of Civil, Environmental and Mechanical Engineering, University of Trento, Via Mesiano 77, 38123 Trento, Italy

3 School of Engineering and Materials Science, Queen Mary University of London, Mile End Road, London E1 4NS, UK

4 Ket-Lab, Edoardo Amaldi Foundation, Via del Politecnico snc, 00133 Rome, Italy

nonlinear response) of nanowire-polymer composite sensors by analyzing the percolation network of nanowires. As an extension of such endeavor, the present study investigates the effect of nanowire orientation distribution in further detail. Since nanowires are embedded in thin nanowire-polymer film in most stretchable sensor applications, instead of having random orientation distribution over full solid angle, nanowire has a limited range of polar angle around 90° (Here, we choose the surface normal vector of thin film as the zenith direction). We find that the gauge factor (relative resistance change over applied mechanical strain) decreases if narrow polar angle distribution is given. We then study the effect of nanowire alignment on the piezoresistive response, by assuming axisymmetric orientation distribution along the tensile direction. We show that a wide range of the gauge factor, from negative to positive, appears as the initial axisymmetric alignment angle varies, and explain such response by analyzing the electrical path change through nanowires. We then compare the numerical results based on percolation network analysis with the prediction of homogenization theory and show that simple analytical prediction based on homogenization theory can be used for the high volume fraction in the linear response regime.

Methods

We build a Matlab-based numerical analysis tool for recognizing the percolation network and calculating the resistance of the percolation network for a nanowire network depicted in Fig. 1a. The simulation code is composed of the following three parts.

Material Properties and the Dimension of the Simulation Cell

The first section defines physical constants, material properties, and geometric properties. All nanowires are assumed to have the same dimension, with its diameter $D = 175$ nm and length $L = 15000$ nm (aspect ratio $(AR) = 85.7$) and we choose the resistivity of silver $1.59 \times 10^{-8}\ \Omega \cdot$ m. Polymer matrix has a dimension of [62.5 μm × 60 μm × 8 μm] while its material properties are given as Poisson's ratio 0.5 (i.e. zero compressibility and volume conservation) and zero conductivity. Perfect adhesion between the nanowires and the matrix is assumed neglecting interfacial debonding by interfacial stress [20]. Since the young's modulus of the silver nanowire is a few orders of magnitude higher than those of polymers, the stretch of the nanowire is neglected and affine transformation is assumed for orientation and center of mass positions of nanowires [11, 18]. We expect that a small fraction of nanowires deforms plastically, but the effect on the overall conductivity would be negligible. Since we assume affine transformation, we do not need to consider Young's moduli of nanowire and polymer. We take the materials' parameters and geometrical parameters from the experimental values of a previous study [17]. Yet, the qualitative conclusion obtained from the present study (the relative change of piezoresistivity upon orientation distribution change) is applicable to a piezoresistive sensor with different materials and geometrical properties. In the initial configuration, nanowires are distributed according to the orientation distributions considered in the following section, while overlaps among different nanowires are allowed for the simplicity [21].

Updating Nanowire Positions Under Uniaxial Loading

Positions of each nanowire inside the matrix are updated with tensile stretching along the x-axis by affine transformation as follow,

$$[x_c, y_c, z_c] = \left[(1+\varepsilon)x_{c0}, \frac{y_{c0}}{\sqrt{(1+\varepsilon)}}, \frac{z_{c0}}{\sqrt{(1+\varepsilon)}}\right] \tag{1}$$

$$\theta = \tan^{-1}\left[\tan\theta_0 \frac{1}{(1+\varepsilon)\sqrt{1+\varepsilon}}\right], \phi = \tan^{-1}\left[\tan\phi_0 \frac{\sin\theta_0}{\sin\theta}\right] \tag{2}$$

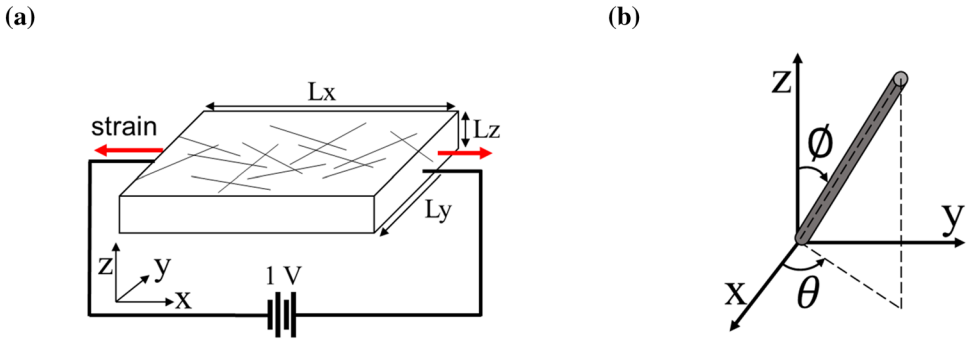

Fig. 1 **a** Configuration of nanowire embedded piezoresistive strain sensor. **b** Configuration of a coordinate system in modeling the nanowire network

where $[x_{c0}, y_{c0}, z_{c0}]$ and $[x_c, y_c, z_c]$ are the center position of each nanowire before and after deformation respectively, $[\theta_0, \phi_0]$ and $[\theta, \phi]$ are azimuthal and polar angles of a spherical coordinate system before and after deformation, respectively, as shown in Fig. 1b. Nanowires tend to align with the x-axis upon tensile stretching. We design the simulation code to enable or disable the periodic boundary conditions along the y and z axes.

After each incremental stretch, we compute the minimum distance (d) between all pairs of nanowires and locate the points where each nanowire meets with the minimum distance line connecting another nanowire. Following the previous study [21], the contact resistance between a pair of nanowires is defined as a function of the minimum distance (d) between the nanowires, as below

$$R = \begin{cases} R_c & (d < d_c) \\ R_c + R_t & (d_c < d < d_t) \\ \infty & (d > d_t) \end{cases} \tag{3}$$

$$\text{where} \quad R_t = \frac{h^2 d_{nm}}{Area \times q^2 \sqrt{2m\lambda}} e^{\left(4\pi d \times d_{nm} \frac{\sqrt{2m\lambda}}{h}\right)}, d_{nm} = d - d_c \tag{4}$$

where R_c is contact resistance, R_t is tunneling resistance, $d_c = D$ is contact cutoff distance, and $d_t = 10D$ is tunneling cutoff distance. h is the Planck constant, q is the electron charge, λ is tunneling energy barrier, m is the electron mass, d_{nm} is distance excluding contact cutoff, $Area$ is the cross-section of the nanowire. The contact condition considered in this study is visualized in Fig. 2.

Recognizing the Percolation Network and Calculating the Resistance of the Network

The depth-first search (DFS) algorithm is employed to identify the percolation network of nanowires connected through either contact resistance or tunneling resistance. DFS is a search algorithm that starts at the root and explores the linked clusters of nanowire members as shown in Fig. 3. After recognizing the clusters touching the left and right ends of the matrix, we calculate the resistance by computing the current flowing through the percolation network. The points of each nanowire that meet with the minimum distance line with another nanowire are considered as the nodes of the network. When V_i is the electronic potential level of i-th node and there are n nodes connected to the i-th node, Kirchhoff's first law is written as below.

$$\sum I = \frac{V_1 - V_i}{R_1} + \frac{V_2 - V_i}{R_2} + \frac{V_3 - V_i}{R_3} + \frac{V_n - V_i}{R_n} = 0 \tag{5}$$

$$\frac{V_1}{R_1} + \frac{V_2}{R_2} + \frac{V_3}{R_3} + \cdots + \frac{V_n}{R_n} - V_i\left(\frac{1}{R_1} + \frac{1}{R_2} + \frac{1}{R_3} + \cdots + \frac{1}{R_n}\right) = 0 \tag{6}$$

$$A_{i1}V_1 + A_{i2}V_2 + A_{i3}V_3 + \cdots + A_{in}V_n - A_{ii}V_i = 0 \tag{7}$$

$$A_{ij} = \frac{1}{R_j}, A_{ii} = \frac{1}{R_1} + \frac{1}{R_2} + \frac{1}{R_3} + \cdots + \frac{1}{R_n} \tag{8}$$

We assign nodes touching the left end of the matrix to have 0 V and nodes touching the right end of the matrix to have 1 V. When k-th node is those touching node, every

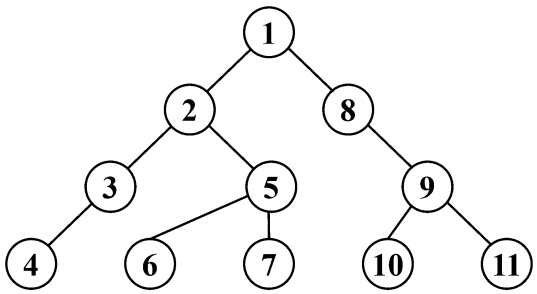

Fig. 3 Configuration of depth-first search (DFS) representing a searching sequence

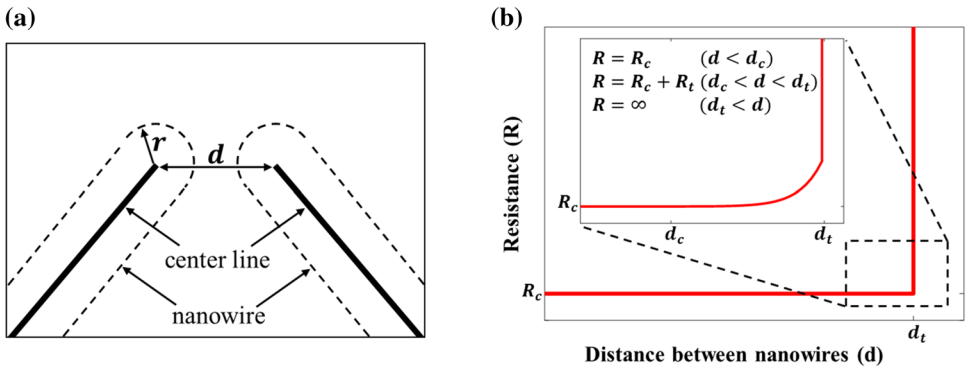

Fig. 2 **a** Configure of modeling nanowire and distance definition between a pair of nanowires. **b** Contact resistance depending on the distance between a pair of nanowires

component of k-th row of matrix $\boldsymbol{A}$ is zero except A_{kk} which is one, and k-th component of vector $\boldsymbol{B}$ has a value of assigned voltage. Components of vector $\boldsymbol{B}$ other than touching nodes are zero. Then we solve the coupled linear equation from Kirchhoff's law by considering the matrix equation $\boldsymbol{AV}=\boldsymbol{B}$. Since we know all of the information of the resistance between nodes which constitute matrix $\mathbf{A}$, the column vector $\boldsymbol{V}$ representing the voltage of each node can be obtained by solving the equation $\boldsymbol{V}=\boldsymbol{A}^{-1}\boldsymbol{B}$. With the voltages in all nodal points, we can compute the current flowing within each link as well as the total current flowing through a percolation network. Finally, the total resistance is calculated from the total current and a voltage difference assigned to the matrix, i.e. 1 V. Nanowire which has more than two nodes with different voltage levels is defined as current flowing nanowires. The above process is repeated after each incremental strain. The resistance of nanowire network, the position and orientation of all nanowire, and the classification of nanowires (current flowing or not) are tracked upon stretching, which is used to create OVITO [22] input files for visualization as depicted in Fig. 4. Here, the red lines represent current flowing nanowires, the blue lines represent percolating nanowires without current flowing, and the black lines represent disconnected nanowires.

Result

The Case with Fully Random Orientation Distribution

Prior to testing the effect of nontrivial orientation distribution, we consider the case with a fully random orientation distribution as a reference. To assign uniform distribution over the entire solid angle, distribution of θ, ϕ, $[x_c, y_c, z_c]$ is given as below

$$\theta = 2\pi u, \phi = \cos^{-1}(2v-1)(0 \le u \le 1, 0 \le v \le 1) \tag{9}$$

$$[x_c, y_c, z_c] = [Lx * a, Ly * b, Ly * c] \tag{10}$$

$$(-0.5 \le a \le 0.5, -0.5 \le b \le 0.5, -0.5 \le c \le 0.5) \tag{11}$$

where u, v, a, b, and c are random variables, and [Lx, Ly, Lz] is the size of the matrix. R_c is assumed to be zero as contact resistance barely affects the behavior of relative resistance change upon stretching [11]. We note that the percolation threshold volume fraction ϕ_C for slender nanowires with fully random orientation is given as follows [11],

$$\phi_C = \frac{1}{8+AR}. \tag{12}$$

For the aspect ratio of nanowires considered in the present study, the percolation threshold ϕ_C is about 1.06%. Although the gauge factor can be maximized around the percolation threshold, the stretchability (i.e. the ability to keep positive electric conductance under tension) would be significantly limited. Hence, in the present study, we consider the volume fraction much higher than ϕ_C, ranging from 2 to 5%. Figure 5 shows the relative resistance change averaged over 10 different initial configurations with different volume fractions. As shown before [11], the relative resistance change is linearly proportional to strain in the small strain regime and is nonlinearly increasing over a certain strain level. This transition from linear behavior to nonlinear behavior occurs when the network topology of a percolating cluster changes from homogeneous to an inhomogeneous configuration with the emergence of a bottleneck in the electrical path [11]. In that context, it is obvious that the transition point is delayed with a higher volume fraction. Also, the relative resistance change over strain (gauge factor) becomes smaller as the volume fraction increases, while the reproducibility (the invariance over different initial configuration with a given volume fraction) increases with volume fraction. Because the main purpose of the present study is the investigation of the orientation distribution effect, we choose the 4% of the volume fraction for all cases considered in the following sections.

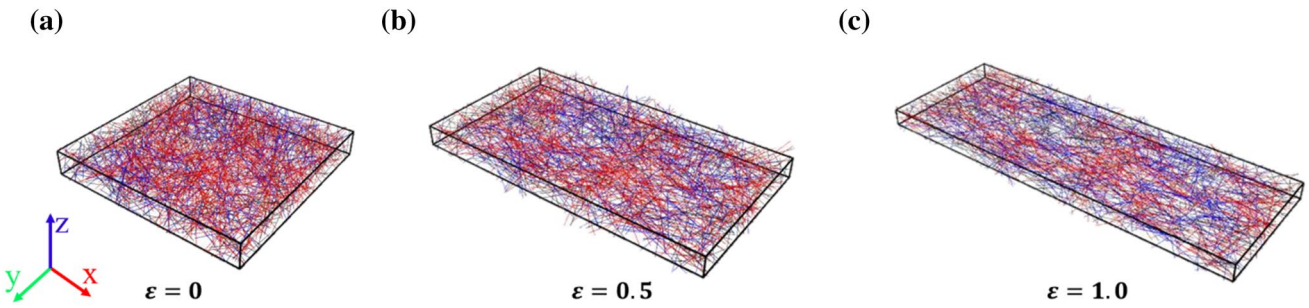

Fig. 4 Sensor configuration visualized by using the OVITO program. Red, blue, and black lines present current flowing nanowires, percolating nanowires without current flowing, and disconnected nanowires. **a** 0% strain **b** 50% strain **c** 100% strain

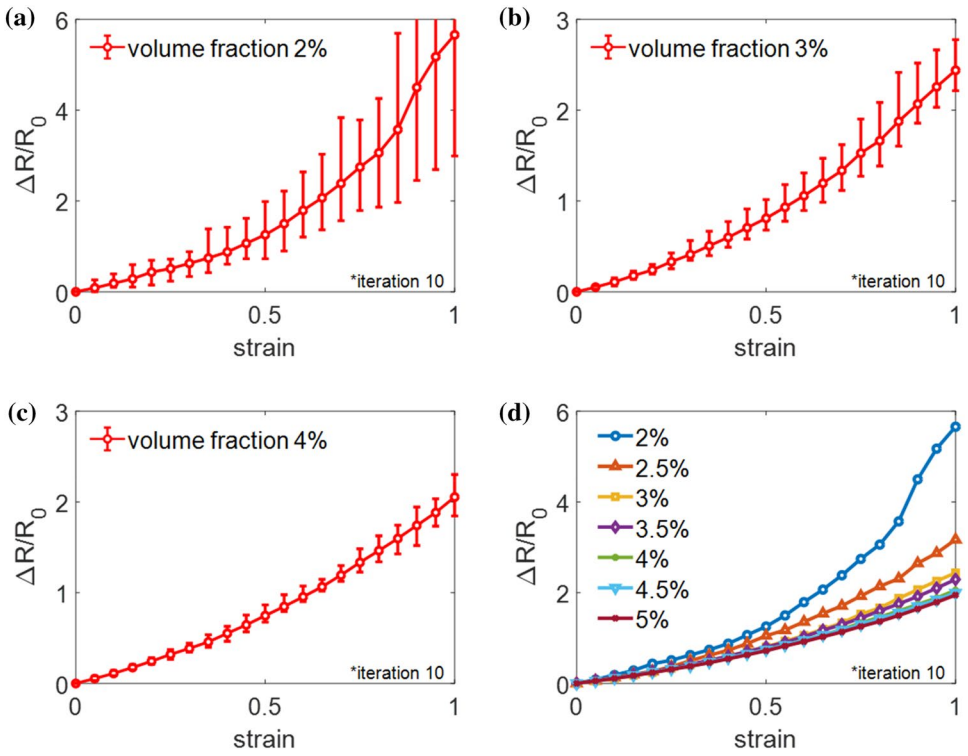

Fig. 5 Behavior of relative resistance for **a** 2%, **b** 3%, **c** 4% of volume fraction. Averaged value over 10 times of iteration and variation are presented. **d** The behavior of average relative resistance over 10 times of iteration at different volume fractions

The Case with Limited Polar Angle Distribution

Since nanowires are embedded in thin nanowire-polymer film in most stretchable sensor applications, instead of having random orientation distribution over full solid angle, nanowire has a limited range of polar angle ϕ around 90°, as depicted in Fig. 6a. To apply a limit on angle ϕ, $\gamma(=\pi/2-\phi)$ is defined as an angle between the xy-plane and nanowire and the distribution of θ and γ is as below

$$\theta = 2\pi u, \gamma = \sin^{-1}[k(2v-1)], (0 \le u \le 1, 0 \le v \le 1, 0 \le k \le 1) \quad (13)$$

where u and v are random variables and k is a factor limiting the maximum magnitude of γ. Figure 6b plots the average relative resistance change in terms of the maximum value γ_{max} at a given volume fraction of 4%. The case with $\gamma_{max} = 90°$ corresponds to the full random distribution, while the case with $\gamma_{max} = 0°$ corresponds to the nanowires oriented perfectly orthogonal to the surface normal vector. We note that $\gamma_{max} = 0°$ case does not correspond to the 2D network because nanowires can have different locations along the z-axis. When γ_{max} is 60°, the result is almost identical to the $\gamma_{max} = 90°$. With a further decrease in γ_{max}, the gauge factor increases monotonically until $\gamma_{max} = 0$. This result indicates that the gauge factor of a piezoresistive sensor based on nanowire-polymer composite with a given volume fraction can be increased by making the initial nanowire orientation distribution as sharp as possible in terms of polar angle.

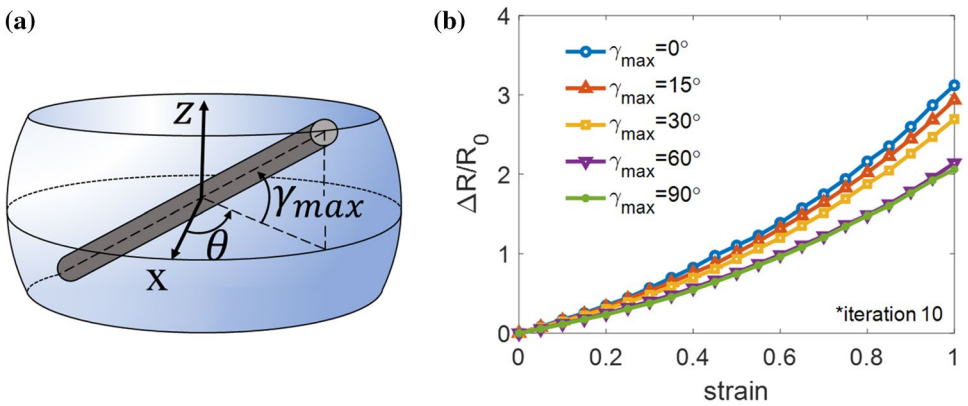

Fig. 6 **a** Configuration of the limited polar angle distribution. **b** Behavior of average relative resistance over 10 times of iteration with the different limits of polar angle at 4% of volume fraction

The Case with Axisymmetric Alignment Along the Loading Direction

We have shown that the partial alignment along the loading direction can lead to a variety of gauge factor with the same volume fraction, in the previous study [11]. Especially, we showed that the negative gauge factor can appear when nanowires are aligned having a large angle with the loading direction. Here, to deepen the understanding of the negative gauge factor, we investigate the initial orientation distribution of nanowires having a fixed angle θ_x with the loading direction and a random angle α (the orientation of projected nanowire on yz-plane) as depicted in Fig. 7a. For various initial θ_x values over a certain threshold, the gauge factor in the small strain regime turns out to be negative but increases with the strain because nanowires align further with the strain as shown in Fig. 7b. The response of a realistic partially aligned nanowire network will be the averaged response of the idealized cases considered here.

The observation from simulations can be explained by a simple analytical model. We consider a pair of nanowires on a plane as depicted in Fig. 8 and change of the electric path upon affine transformation. Upon strain increment, the distance between centroid positions of two nanowires always increases in proportion to the strain, while the tips of nanowires may bet closer if the initial angle θ_0 is large enough to overcome the centroid motion (we note that the rotation angle of nanowires gets larger for larger θ_0 from Eq. (2)). The new alignment angle θ can be obtained in terms of applied strain ε and initial angle θ_0, as from Eq. (2). Then, the resistance between two centroid points of initially touching nanowire pair can be written as follows

$$R = 2r_0 l = \frac{r_0 h(1+\varepsilon)}{\cos\theta} = \frac{r_0 h}{\cos\theta}\left(\frac{tan\theta_0}{tan\theta}\right)^{\frac{2}{3}} \tag{14}$$

where r_0 is resistance per unit length of the nanowire. The negative gauge factor threshold can be obtained from the point where a relative change of resistance over the current alignment angle θ becomes zero, i.e. $\frac{dR}{d\theta} = 0$. We found that $\frac{dR}{d\theta} = 0$ condition is met when $\theta = \cos^{-1}\left(\frac{1}{3}\right) = 54.74°$. From Eq. (2), we can obtain the initial alignment angle θ_0 to have zero piezoresistive response at strain ε. For example, to have zero gauge factor at initial stretching, $\theta_0 = 54.74°$ is needed, and the relative resistance change increases with strain. On the other hand, to target zero gauge factor at $\varepsilon = 0.2$, the initial angle $\theta_0 = 61.72°$ is needed. Such nanowire network will have significantly large negative gauge factor at very small strain regime but its tangential gauge factor (or instantaneous gauge factor), defined as $\frac{dR/R}{d\varepsilon}$, becomes zero near $\varepsilon = 0.2$. We summarize the prediction from the simple calculations in Table 1, and despite of very simple assumption, our prediction matches qualitatively with the results from Fig. 7b.

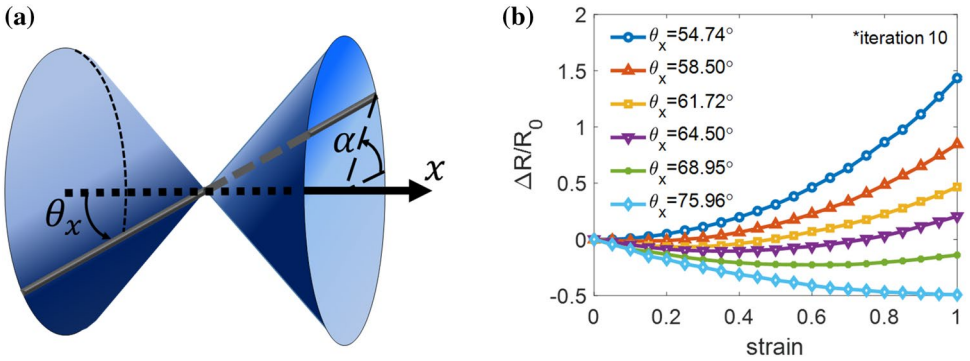

Fig. 7 **a** Configuration of the axisymmetric alignment along the loading direction. **b** Behavior of average relative resistance over 10 times of iteration for different fixed angles with loading direction for the axisymmetric alignment distribution case. The volume fraction of nanowires is 4%

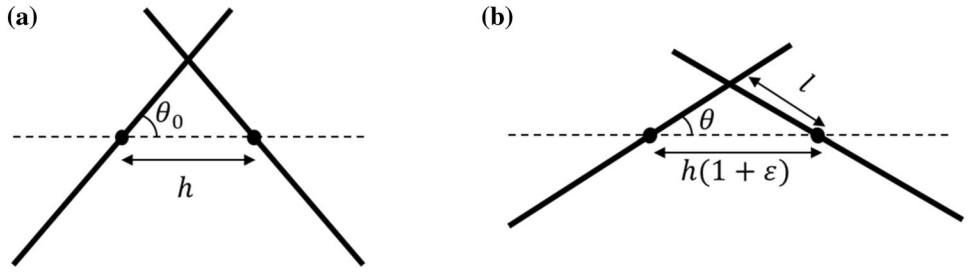

Fig. 8 Configuration of the affine transformation of a pair of nanowires on a plane. **a** Reference position. **b** Affine transformed position

Table 1 Comparing the critical strain from prediction and simulation upon initial θ_x

Initial θ_x	Critical strain in prediction	Critical strain in simulation	Minimum relative R value
54.74°	0.0	0.05	− 0.000354
58.50°	0.1	0.1	− 0.01605
61.72°	0.2	0.25	− 0.06569
64.50°	0.3	0.35	− 0.1046
68.95°	0.5	0.6	− 0.2263
75.96°	1.0	1.25	− 0.4999

Minimum relative resistance for each initial θ_x is obtained from averaged simulation results

Comparison with the Prediction of Homogenization Theory

Effective resistance for nanowire embedded rubber can be predicted by mean-field homogenization theory for computing the effective conductivity of composites. Technically, homogenization theory is applicable to obtain the conductivity of composite involving sparsely dispersed nanowires that do not form percolation network and also does not account for the topology change of a percolation network. Yet, it may give a first-order approximation on the gauge factor in the limit of large volume fraction and small strain where the topology of the percolation network does not change significantly. According to the Mori–Tanaka mean-field approximation, the conductivity of nanowire-polymer network is given as follows [23–27],

$$\boldsymbol{L}_{eff} = \left(c_0\boldsymbol{L}_0 + c_1\langle \boldsymbol{L}_1\boldsymbol{A}\rangle\right)\left(c_0\boldsymbol{I} + c_1\langle \boldsymbol{A}\rangle\right)^{-1} \tag{15}$$

$$\text{where} \quad \mathbf{A} = \left[\boldsymbol{I} + \boldsymbol{S}\boldsymbol{L}_0^{-1}\left(\boldsymbol{L}_1 - \boldsymbol{L}_0\right)\right]^{-1} \tag{16}$$

$$< X >_{ij} = \frac{\int_0^{\frac{\pi}{2}}\int_{-\pi}^{\pi} X'_{ij}(\theta,\phi)\lambda(\phi)\sin(\phi)d\theta d\phi}{\int_0^{\frac{\pi}{2}}\int_{-\pi}^{\pi}\lambda(\phi)\sin(\phi)d\theta d\phi} \tag{17}$$

$$X'_{ij} = C_{ip}C_{jq}X_{pq} \quad \text{where} \quad \boldsymbol{C} = \begin{bmatrix} cos\theta & -sin\theta & 0 \\ sin\theta cos\phi & cos\theta cos\phi & -sin\phi \\ sin\theta\sin\phi & cos\theta sin\phi & cos\phi \end{bmatrix} \tag{18}$$

where $\boldsymbol{L}_0$, $\boldsymbol{L}_1$, $\boldsymbol{L}_{eff}$ are 3×3 conductivity matrix of the matrix, nanowire, and the composite, respectively. c_0 and c_1 are volume fraction of the matrix and nanowires, respectively. $\boldsymbol{S}$ is Eshelby tensor, $\boldsymbol{I}$ is an identity matrix, and $\lambda(\phi)$ is orientation distribution function. We note that the nonzero conductivity can be obtained only if we assume a nonzero conductivity of the matrix. Thus, we assign very small conductivity to the matrix and obtain the resistance change over strain by accounting the change of nanowire orientation distribution in the orientation (see supplementary note for detail of orientation distribution change). We found that the analytical prediction from micromechanics does not match

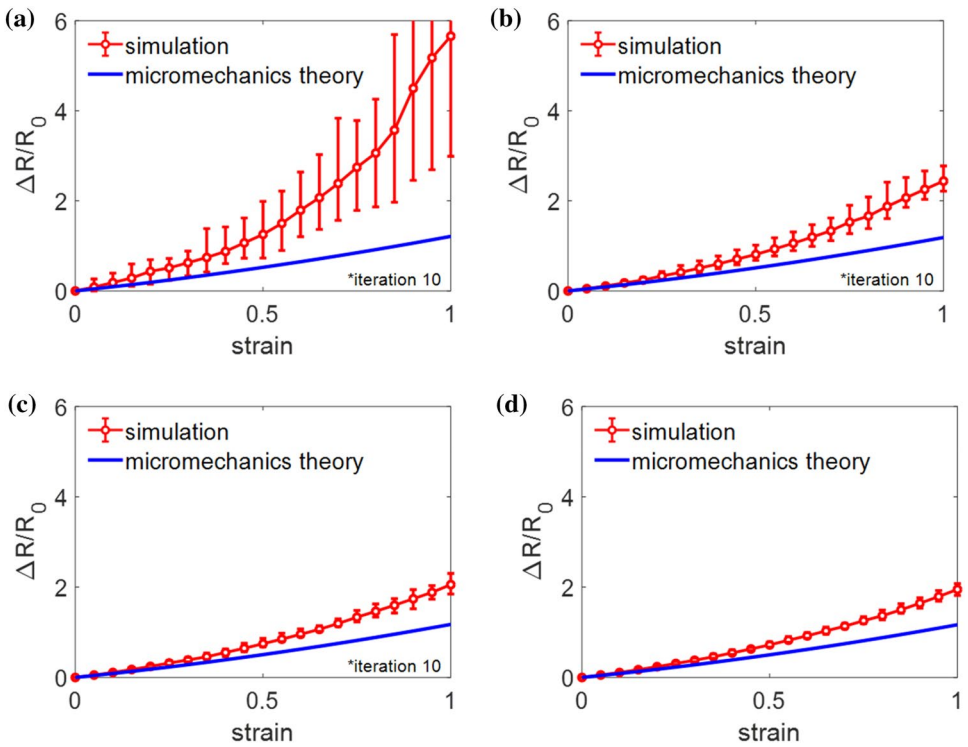

Fig. 9 Comparing results of simulation and homogenization theory at volume fraction of **a** 2% **b** 3% **c** 4% **d** 5%. The results of the simulation are obtained from 10 times of iteration and averaged

with the numerical results in the entire range of strain if the initial volume fraction is 2–3%. In this case, the percolation network topology (the number of nodes and connected links) changes significantly upon the small stretch. However, for the higher volume fraction of 4–5%, the micromechanics prediction turns out to match reasonably well with the numerical results at least in the small strain regime because of stable percolation network topology as shown in Fig. 9. Also, macroscopic stress upon the strain can be obtained using a homogenization method [28]. Overall, we find that micromechanics can be used in the linear response regime of the composites with high volume fractions.

Conclusion

In the present study, we investigate the effect of orientation distribution on the piezoresistivity of nanowire-polymer composite, based on a numerical simulation tool for modeling the percolation network. We find that, given a volume fraction, the piezoresistive sensitivity of the composite can be maximized if nanowires are perfectly oriented orthogonal to surface normal vector of the thin film. We also investigate the negative piezoresistive response for nanowires aligned almost orthogonal to the loading direction in detail, and explained the mechanism behind the negative and zero piezoresistive responses. Finally, we compare the results from the numerical simulation with the analytical prediction from homogenization theory and find that homogenization theory can be used to estimate the piezoresistive response of a composite with high volume fraction (4–5%) in a small strain regime.

Acknolwedgements This research was supported by the Basic Science Program (NRF-2019R1A2C4070690) of the National Research Foundation of Korea (NRF) funded by the Ministry of Science and ICT of Korea. N.M.P. is supported by the European Commission under the Graphene Flagship Core 2 grant No. 785219 (WP14, "Composites"), the FET Proactive ("Neurofibres") grant No. 732344, the FET Open (Boheme) grant No. 863179 as well as by the Italian Ministry of Education, University and Research (MIUR) under the "Departments of Excellence" grant L. 232/2016, the ARS01- 01384-PROSCAN and the PRIN-20177TTP3S grants."

Compliance with Ethical Standards

Conflict of Interest The authors declare no competing interests.

References

1. T. Yamada, Y. Hayamizu, Y. Yamamoto, Y. Yomogida, A. Izadi-Najafabadi, D.N. Futaba, K. Hata, A stretchable carbon nanotube strain sensor for human-motion detection. Nat. Nanotechnol. **6**(5), 296–301 (2011)
2. I. Kang, M.J. Schulz, J.H. Kim, V. Shanov, D. Shi, A carbon nanotube strain sensor for structural health monitoring. Smart Mater. Struct. **15**(3), 737–748 (2006)
3. C. Liu, J. Choi, An embedded PDMS nanocomposite strain sensor toward biomedical applications, in: 2009 Annual International Conference of the IEEE Engineering in Medicine and Biology Society, pp. 6391–6394 (2009)
4. F. Lorussi, S. Enzo Pasquale, M. Tesconi, A. Tognetti, D.D. Rossi, Strain sensing fabric for hand posture and gesture monitoring. IEEE Trans. Inf. Technol. Biomed. **9**(3), 372–381 (2005)
5. T. Giorgino, P. Tormene, F. Lorussi, D.D. Rossi, S. Quaglini, Sensor evaluation for wearable strain gauges in neurological rehabilitation. IEEE Trans. Neural Syst. Rehabil. Eng. **17**(4), 409–415 (2009)
6. J. Zhang, J. Liu, R. Zhuang, E. Mäder, G. Heinrich, S. Gao, Single MWNT-glass fiber as strain sensor and switch. Adv. Mater. **23**(30), 3392–3397 (2011)
7. R.J.N. Helmer, D. Farrow, K. Ball, E. Phillips, A. Farouil, I. Blanchonette, A pilot evaluation of an electronic textile for lower limb monitoring and interactive biofeedback. Proc. Eng. **13**, 513–518 (2011)
8. C.-X. Liu, J.-W. Choi, Patterning conductive PDMS nanocomposite in an elastomer using microcontact printing. J. Micromech. Microeng. **19**(8), 085019 (2009)
9. N. Lu, C. Lu, S. Yang, J. Rogers, Highly sensitive skin-mountable strain gauges based entirely on elastomers. Adv. Funct. Mater. **22**(19), 4044–4050 (2012)
10. X. Xiao, L. Yuan, J. Zhong, T. Ding, Y. Liu, Z. Cai, Y. Rong, H. Han, J. Zhou, Z.L. Wang, High-strain sensors based on ZnO nanowire/polystyrene hybridized flexible Films. Adv. Mater. **23**(45), 5440–5444 (2011)
11. S. Lee, M. Amjadi, N. Pugno, I. Park, S. Ryu, Computational analysis of metallic nanowire-elastomer nanocomposite based strain sensors. AIP Adv. **5**(11), 117233 (2015)
12. H. Souri, J. Yu, H. Jeon, J.W. Kim, C.-M. Yang, N.-H. You, B.J. Yang, A theoretical study on the piezoresistive response of carbon nanotubes embedded in polymer nanocomposites in an elastic region. Carbon **120**, 427–437 (2017)
13. N. Hu, Y. Karube, M. Arai, T. Watanabe, C. Yan, Y. Li, Y. Liu, H. Fukunaga, Investigation on sensitivity of a polymer/carbon nanotube composite strain sensor. Carbon **48**(3), 680–687 (2010)
14. Y. Wang, G.J. Weng, S.A. Meguid, A.M. Hamouda, A continuum model with a percolation threshold and tunneling-assisted interfacial conductivity for carbon nanotube-based nanocomposites. J. Appl. Phys. **115**(19), 193706 (2014)
15. T.C. Theodosiou, D.A. Saravanos, Numerical investigation of mechanisms affecting the piezoresistive properties of CNT-doped polymers using multi-scale models. Compos. Sci. Technol. **70**(9), 1312–1320 (2010)
16. G. Lee, S.G. Lee, Y. Chung, G.Y. Bae, S. Lee, S. Ryu, K. Cho, Omnidirectionally and highly stretchable conductive electrodes based on noncoplanar zigzag mesh silver nanowire arrays. Adv. Electron. Mater. **2**(8), 1600158 (2016)
17. M. Amjadi, A. Pichitpajongkit, S. Lee, S. Ryu, I. Park, Highly stretchable and sensitive strain sensor based on silver nanowire-elastomer nanocomposite. ACS Nano **8**(5), 5154–5163 (2014)
18. M. Taya, W.J. Kim, K. Ono, Piezoresistivity of a short fiber/elastomer matrix composite. Mech. Mater. **28**(1), 53–59 (1998)
19. I. Chung, M. Cho, Recent studies on the multiscale analysis of polymer nanocomposites. Multiscale Sci. Eng. **1**(3), 167–195 (2019)
20. F. Gou, C. Ke, Theoretical predictions of the interfacial stress transfer in nanotube-reinforced polymer nanocomposites by using a strain-hardening shear-lag model. Multiscale Sci. Eng. **1**(3), 236–246 (2019)

21. N. Hu, Y. Karube, C. Yan, Z. Masuda, H. Fukunaga, Tunneling effect in a polymer/carbon nanotube nanocomposite strain sensor. Acta Mater. **56**(13), 2929–2936 (2008)
22. A. Stukowski, Visualization and analysis of atomistic simulation data with OVITO–the open visualization tool. Model. Simul. Mater. Sci. Eng. **18**(1), 015012 (2009)
23. S. Lee, S. Ryu, Theoretical study of the effective modulus of a composite considering the orientation distribution of the fillers and the interfacial damage. Eur. J. Mech. A. Solids **72**, 79–87 (2018)
24. T. Mori, K. Tanaka, Average stress in matrix and average elastic energy of materials with misfitting inclusions. Acta Metall. **21**(5), 571–574 (1973)
25. Y. Benveniste, A new approach to the application of Mori-Tanaka's theory in composite materials. Mech. Mater. **6**(2), 147–157 (1987)
26. G.M. Odegard, T.S. Gates, K.E. Wise, C. Park, E.J. Siochi, Constitutive modeling of nanotube–reinforced polymer composites. Compos. Sci. Technol. **63**(11), 1671–1687 (2003)
27. N. Marzari, M. Ferrari, Textural and micromorphological effects on the overall elastic response of macroscopically anisotropic composites. J. Appl. Mech. **59**(2), 269–275 (1992)
28. D.A. Colera, H.-G. Kim, Asymptotic expansion homogenization analysis using two-phase representative volume element for non-periodic composite materials. Multiscale Sci. Eng. **1**(2), 130–140 (2019)

Supplementary material

Orientation distribution dependence of piezoresistivity of metal nanowire – polymer composite

Jiyoung Jung[1], Sangryun Lee[1], Nicola M. Pugno[2,3,4], and Seunghwa Ryu[1,*]

Affiliations

[1]Department of Mechanical Engineering, Korea Advanced Institute of Science and Technology (KAIST), 291 Daehak-ro, Yuseong-gu, Daejeon 34141, Republic of Korea

[2]Laboratory of Bio-Inspired and Graphene Nanomechanics, Department of Civil, Environmental and Mechanical Engineering, University of Trento, via Mesiano 77, I-38123 Trento, Italy
[3]School of Engineering and Materials Science, Queen Mary University of London, Mile End Road, E1 4NS London, United Kingdom
[4]Ket-Lab, Edoardo Amaldi Foundation, via del Politecnico snc, I-00133 Roma, Italy

*Corresponding author e-mail: ryush@kaist.ac.kr

Supplementary Note: Orientation distribution change

We analytically derived angle distribution change depending on strain as follows,

$f(\theta_x) = f[\cos^{-1}(\sin\emptyset\cos\theta)]$

$f(\theta) = \frac{1}{2\pi},\ \theta \in [-\pi, \pi]$ set distribution function for θ

$f(\emptyset) = \frac{1}{2}\sin\phi,\ \phi \in [0, \pi]$ set distribution function for ϕ

$$f(\cos\theta) = \sum_{\cos\theta=y} f_\theta(\cos^{-1} y)\left|\frac{d\theta}{dy}\right| = \sum_{\cos\theta=y} \frac{1}{2\pi}\left|\frac{-1}{\sqrt{1-y^2}}\right| = \frac{1}{\pi\sqrt{1-y^2}}, \qquad y \in [-1,1]$$

$$f(\cos\theta) = \frac{2}{\pi\sqrt{1-y^2}}\ y \in [0,1]\ (\because symmetry)$$

$$f(\sin\phi) = \sum_{\sin\emptyset=z} f_\emptyset(\sin^{-1} z)\left|\frac{d\phi}{dz}\right| = \sum_{\sin\phi=z} \frac{1}{2} z\left|\frac{1}{\sqrt{1-z^2}}\right| = \frac{z}{\sqrt{1-z^2}}, \qquad z \in [0,1]$$

$$f(\sin\phi\cos\theta) = \int_{-\infty}^{\infty} f_Y\left(\frac{p}{z}\right) f_z(z)\frac{1}{|z|}dz = \int_p^1 \frac{2}{\pi}\frac{1}{\sqrt{1-\frac{p^2}{z^2}}}\frac{z}{\sqrt{1-z^2}}\frac{1}{|z|}dz = 1, \qquad p \in [0,1]$$

$\theta_x = \cos^{-1} p$

$$f(\theta_x) = \sum_{\cos\varphi=p} f_p(\cos\theta_x)\left|\frac{dp}{d\theta_x}\right| = \sin\varphi, \qquad \varphi \in \left[0, \frac{\pi}{2}\right]$$

$q = \tan\theta_x$

$$f(\tan\theta_x) = \sum_{\tan\varphi=q} f_{\theta_x}(\tan^{-1} q)\left|\frac{d\theta_x}{dq}\right| = \frac{q}{\sqrt{q^2+1}}\frac{1}{q^2+1}, \qquad q \in [0,\infty]$$

$$\theta_x' = \tan^{-1}\left[\tan\theta_x \frac{1}{(1+\varepsilon)\sqrt{1+\varepsilon}}\right]$$

$$f\left(\tan\theta_x \frac{1}{(1+\varepsilon)\sqrt{1+\varepsilon}}\right) = \frac{(1+\varepsilon)^3 q}{\sqrt{(1+\varepsilon)^3 q^2+1}[(1+\varepsilon)^3 q^2+1]}, \quad q \in [0,\infty]$$

$$f(\theta_x') = f\left(\tan^{-1}\left[\tan\theta_x \frac{1}{(1+\varepsilon)\sqrt{1+\varepsilon}}\right]\right) = \frac{(1+\varepsilon)^3\tan x\sec^2 x}{\sqrt{(1+\varepsilon)^3\tan^2 x+1}[(1+\varepsilon)^3\tan^2 x+1]}$$

$$\frac{f(\theta_x')}{\sin\theta_x} = \frac{(1+\varepsilon)^3\tan x\sec^2 x}{\sqrt{(1+\varepsilon)^3\tan^2 x+1}[(1+\varepsilon)^3\tan^2 x+1]}\frac{1}{\sin x}\frac{1}{\int_0^{\frac{\pi}{2}}\frac{f(\theta_x')}{\sin\theta_x}dx}, \quad x \in [0,\frac{\pi}{2}]$$

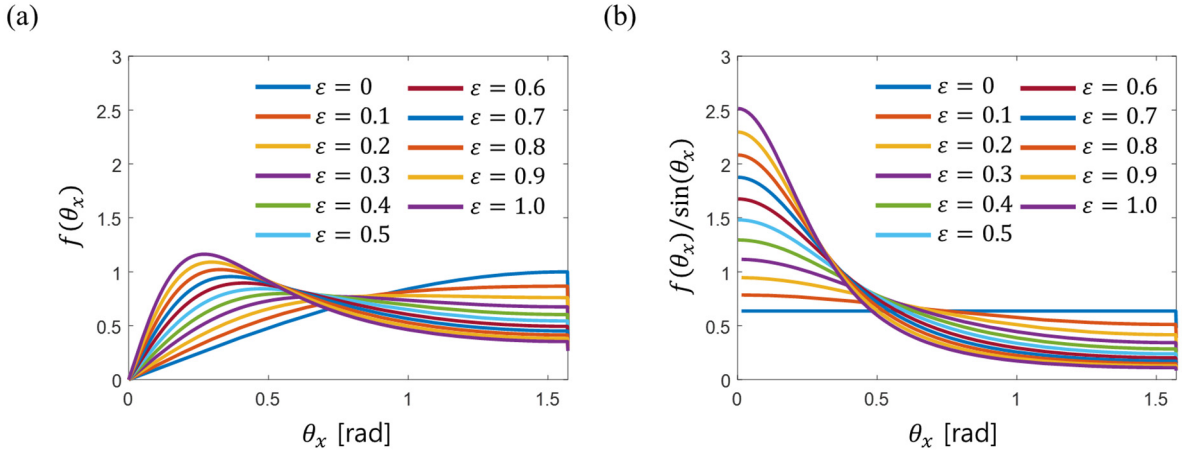

Figure S.1. The probability distribution function of the polar angle with loading direction depending on the strain. Reference distribution at zero strain ($\boldsymbol{\varepsilon}$=0).